

Fall-Off Curves for the Reaction $\text{ClO} + \text{NO}_2 (+\text{N}_2) \rightarrow \text{ClONO}_2 (+\text{N}_2)$

Reinhard Zellner

Institut für Physikalische Chemie der Universität Göttingen, Göttingen, West Germany

(Z. Naturforsch. **32 a**, 648–651 [1977]; received May 11, 1977)

Fall-off curves for the reaction $\text{ClO} + \text{NO}_2 (+\text{N}_2) \rightarrow \text{ClONO}_2 (+\text{N}_2)$ at 300 and 220 K have been calculated from Kassel integrals by use of a theoretically derived high pressure limit and the experimentally determined low pressure limit as reference points. The reaction is found to deviate considerably from the low pressure limit at pressures larger than 10 Torr. Effective rate constants for the use in atmospheric models of chlorine nitrate formation are derived.

The recombination reaction between ClO and NO_2 has recently¹ received considerable attention in connection with the possible depletion of stratospheric ozone by photochemically initiated reactions of fluorocarbons. Due to the relatively high photolytic stability¹ of the chlorine nitrate product, the effect of this reaction would be to provide a sink for ClO (and simultaneously for NO_2) and to reduce the ClO_x catalytic ozone destruction efficiency. According to a recent comprehensive report² the inclusion of



into the stationary state equation for ClO would reduce the ratio of active to inactive chlorine containing species ($[\text{ClO}]/[\text{ClX}]$) by $\sim 10\%$ in the mid stratosphere. Because of the lower temperature as well as higher pressure the effect would be larger in the lower stratosphere. Correspondingly, ClONO_2 is predicted to exist in the stratosphere with a maximum volume mixing ratio of 5×10^{-10} and a distribution sharply peaked around 25 km².

The quality of such predictions is primarily dependent on the accuracy of the input rate data. Since reaction (1) is a recombination process, its rate constant will depend on pressure, temperature and the nature of the third body M. Consequently, a large body of data is required in order to deduce the effective bimolecular rate constant k_1 for all atmospheric conditions of interest.

At the present time no experimental rate data for reaction (1) except for the low pressure limit (k_1^0)^{3–6} are available. These data have been used in model calculations of the mid stratosphere where

the low pressure limit is the governing kinetic regime. For the lower stratosphere this reaction is expected to be in the kinetic transition region. Rate constants relating to the extent of deviation from the k_1^0 limit with increasing pressure, however, are as yet unavailable.

In the present work the variation of the effective bimolecular rate constant with pressure ('fall-off' curve) is calculated from Kassel integrals⁷. Apart from the ClONO_2 molecular properties this calculation requires a knowledge of the limiting low and high pressure rate constants (k_1^0 and k_1^∞). Whereas the former is available from experiment, the latter had to be calculated independently from current theory⁸. This approach appears as a reasonable combination of experimental information and theoretical prediction. Since it accounts fully for the molecular properties of ClONO_2 , considerable insight into the details of the 'fall-off' behaviour is obtained. This in turn provides a hint as to some ambiguities in the low pressure experimental data. The present work is part of a review on atmospheric recombination reactions⁹.

The Low Pressure Limiting Rate Constant k_1^0

Reaction (1) has been studied recently in three different laboratories using low pressure ($p = 1 - 6$ Torr) flow systems^{3–5}. The results are in remarkable good agreement concerning both, the absolute values and the first-order $[\text{M}]$ dependence. Therefore, at 300 K a low pressure limiting rate constant $k_1^0 (\text{M} = \text{N}_2) = (1.6 \pm 0.2) \times 10^{-31} \text{ cm}^6/\text{molecule}^2 \cdot \text{s}$

can be deduced with some confidence. Temperature dependence measurements of k_1^0 for $\text{M} = \text{He}$ ³ and N_2 ^{4,5} are compiled in Figure 1. Since the range of these studies has been restricted to above 250 K,

Reprint requests to Dr. R. Zellner, Institut für Physikalische Chemie, Universität Göttingen, Tammannstraße 6, D-3400 Göttingen.



Dieses Werk wurde im Jahr 2013 vom Verlag Zeitschrift für Naturforschung in Zusammenarbeit mit der Max-Planck-Gesellschaft zur Förderung der Wissenschaften e.V. digitalisiert und unter folgender Lizenz veröffentlicht: Creative Commons Namensnennung-Keine Bearbeitung 3.0 Deutschland Lizenz.

Zum 01.01.2015 ist eine Anpassung der Lizenzbedingungen (Entfall der Creative Commons Lizenzbedingung „Keine Bearbeitung“) beabsichtigt, um eine Nachnutzung auch im Rahmen zukünftiger wissenschaftlicher Nutzungsformen zu ermöglichen.

This work has been digitalized and published in 2013 by Verlag Zeitschrift für Naturforschung in cooperation with the Max Planck Society for the Advancement of Science under a Creative Commons Attribution-NoDerivs 3.0 Germany License.

On 01.01.2015 it is planned to change the License Conditions (the removal of the Creative Commons License condition "no derivative works"). This is to allow reuse in the area of future scientific usage.

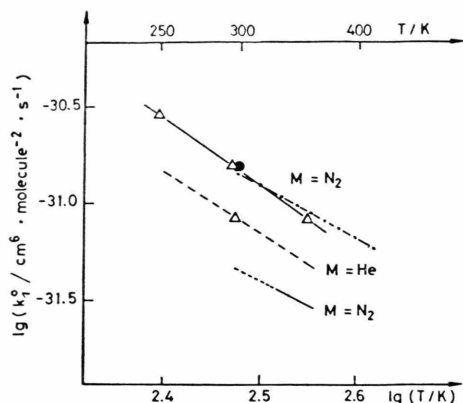


Fig. 1. $\lg k$ vs. $\lg T$ plot of the experimentally determined low pressure rate constant k_1^0 . ---- and ●: Zahniser, Kaufman³; △: Birks et al.⁴; - · - · - · Leu et al.⁵ (measurements for M = He, Ar are omitted); · · · - ·: Knauth⁶ (from reverse dissociation).

rate constants for the lowest atmospheric temperature (220 K) can only be derived by extrapolation. Whereas the data of Birks et al.⁴ and those of Zahniser et al. (taking their data for M = He and assuming an invariance of the temperature dependence on the nature of M) predict a value of k_1^0 (M = N₂) = $(4.9 - 5.1) \times 10^{-31}$, the results of De More and coworkers⁵ show a slightly stronger temperature dependence and yield k_1^0 (M = N₂) = $7 \times 10^{-31} \text{ cm}^6/\text{molecule}^2 \cdot \text{s}$ at 220 K.

In view of this we have accepted k_1^0 (M = N₂) = $5.5 \times 10^{-31} \text{ cm}^6/\text{molecule}^2 \cdot \text{s}$ at 220 K as a reference value to be used in our 'fall-off' calculation.

Further information on the rate of reaction (1) is provided by a study in the range 50–90 °C of the thermal decomposition of chlorine nitrate⁶. When combined with the equilibrium constant¹⁰, these experiments yield a considerably lower k_1^0 (M = N₂) data (cf. Figure 1). According to our 'fall-off' analysis we attribute this partly to a substantial deviation of the pressure range used in these experiments ($p = 20 - 200$ Torr of N₂) from the low pressure limit.

The High Pressure Limit (k_1^∞) and the 'Fall-off' Region

We have calculated the 'fall-off' curve for this reaction in a reduced form (k_1/k_1^∞ as a function of k_1^0/k_1^∞) from Kassel integrals. This method is described fully in Ref. ⁷ and an account of its application to atmospheric recombination reactions is

given in ⁹. Whereas k_1^0 can be taken from experiments (see above) the high pressure limiting rate constant (k_1^∞) is so far only accessible by theoretical prediction.

We have applied the adiabatic channel modification of the maximum free energy concept of transition state theory, recently introduced by Quack and Troe⁸. In this theory the partition function of the dissociating molecule ($Q'_{(q)}$) is calculated as a function of q , the intermolecular separation, for electronic, centrifugal and rovibrational parts separately. The latter contains all vibrations (except the one associated with the reaction coordinate), the external rotation around the axis of fragmentation and possible internal rotations. It is obtained from the rovibrational partition functions of reactant and fragments by exponential interpolation. The total partition function is finally minimized and the (temperature dependent) location of this minimum is identified with the 'transition state'.

Our calculation were done with the following ClONO₂ frequencies (in cm⁻¹) 1292, 1735, 780, 809, 434, 560, 270, 711, 121^{11,12}. Of these, the NO₂ symmetric bending vibration ($\nu_5 = 434 \text{ cm}^{-1}$) was considered as the reaction coordinate mode. The rotational constant A (around the ClO-NO₂ axis) was calculated from the relation $A = B_{\text{ClO}} B_{\text{NO}_2} / (B_{\text{ClO}} + B_{\text{NO}_2})$ to be $A = 0.258 \text{ cm}^{-1}$, where B 's are the corresponding rotational constants for ClO and NO₂, respectively. The torsional mode ($\nu_9 = 121 \text{ cm}^{-1}$) was treated as a vibration throughout, which seems justified on the basis of the relatively large rotational barrier in ClONO₂ of $\sim 32 \text{ kJoule/mol}$ ¹² and the proximity of energy levels of harmonic oscillator and restricted rotator at total energies well below the barrier¹³. The minimization procedure for $Q'_{(q)}$ (with a fixed adiabatic channel parameter $\gamma = 0.75 \text{ \AA}^{-1}$, see ⁸) resulted in a location of the activated complex at $q^\ddagger = 3.0 \text{ \AA}$ at 300 K, more than twice the accepted equilibrium bond length in ClONO₂ of $q_e = 1.41 \text{ \AA}$ ¹². From the corresponding partition function and the equilibrium constant (from Ref. ¹⁰) an absolute value $k_1^\infty = 6.2 \times 10^{-12} \text{ cm}^3/\text{molecule} \cdot \text{s}$ at was obtained. A similar calculation for 220 K resulted in a location of the 'transition state' at slightly larger bond extensions ($q^\ddagger = 3.2 \text{ \AA}$). The derived rate constant, however, showed no important temperature dependence.

Rate constants for the intermediate pressure region were derived from Kassel integrals with k_1^0

and k_1^∞ as reference points. The important quantity in this calculation is the Kassel parameter S_K :

$$[S_K \cong S_{\text{eff}} + 1 \text{ and } S_{\text{eff}} = - (1/T) d \ln Q/d(1/T)]^7.$$

Depending on whether the torsional mode (ν_9) of ClONO_2 is treated as vibration or rotation, S_{eff} is somewhat effected [$S_{\text{eff}} = 1.9$ (1.45) for ν_9 as vibration and 1.23 (0.82) for ν_9 as rotation at 300 K (220 K).] This in turn influences the fall-off characteristics. At low total pressure (i. e. 10 Torr), where the extent of 'fall-off' from first order kinetics is small in the case of rotational treatment of ν_9 (12% at 300 K and $\sim 19\%$ at 220 K) this is almost doubled for a treatment of this motion as vibration. The absolute rate constant $k_1^{(M)}$, however, is only reduced by $\sim 10\%$. Figure 2 represents calculated 'fall-off' curves for 300 and 220 K for $M = \text{N}_2$ (for the case of rotational treatment of ν_9). Weak collision effects are accounted for by assuming a collision efficiency of N_2 of $\beta_c = 0.3$.

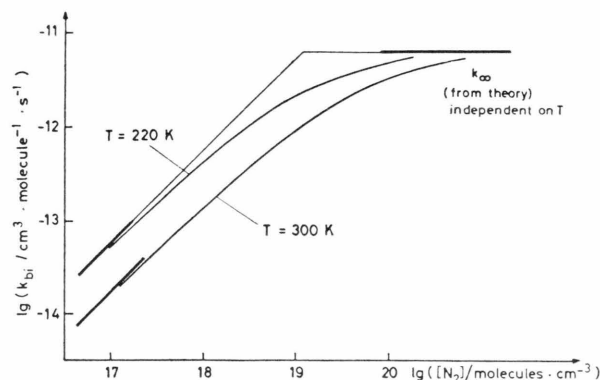


Fig. 2. 'Fall-off' curves for $\text{ClO} + \text{NO}_2 + \text{N}_2 \rightarrow \text{ClONO}_2 + \text{N}_2$ at 300 and 220 K. The low pressure limits are those from Ref. ³⁻⁵ (see text). The torsional mode of ClONO_2 is treated as rotation; $S_K = 2.2$ (1.8) at 300 K (220 K).

It is obvious from this figure that at pressures larger than 10 Torr the reaction clearly occurs in the kinetic transition region. Since in connection with atmospheric chemistry we are primarily concerned with absolute rate constants (rather than precise amounts of 'fall-off') the above distinction between the two treatments of ν_9 is not too important. The 10% difference of $k_1^{(M)}$ is virtually maintained throughout the whole 'fall-off' region. Table I lists effective bimolecular rate constants as a function of stratospheric altitude. Because reaction (1) has been compared to the well investigated ^{14, 15} reaction (2) $\text{OH} + \text{NO}_2 (+\text{N}_2) \rightarrow \text{HNO}_3 (+\text{N}_2)$, effective rate data for the latter process are also presented. Primarily due to the fact that the ratio of the high pressure rate constants ($k_1^\infty/k_2^\infty \sim 0.4$ at 300 K) is larger than that of the low pressure rate constants ($k_1^0/k_2^0 \sim 0.06$ at 300 K and for $M = \text{N}_2$), the listed ratio of the effective rate constants decreases with increasing altitude.

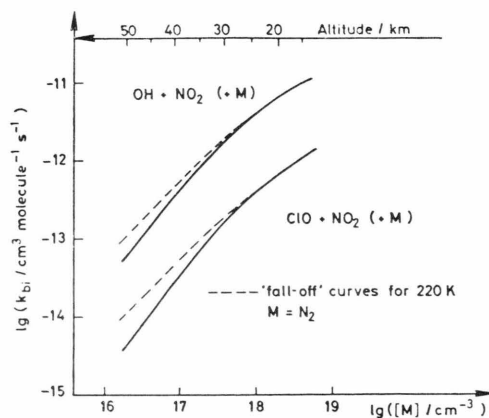


Fig. 3. Effective bimolecular rate constants for the recombination of NO_2 with OH and ClO as a function of stratospheric altitude. The dashed lines are 'fall-off' curves at 220 K for $M = \text{N}_2$.

| Altitude km | <i>p</i> Torr | <i>T</i> K | lg <i>M</i> (cm ⁻³) | $\text{ClO} + \text{NO}_2 (+\text{N}_2)$ $k_{\text{bi}}/\text{cm}^3 \cdot \text{molecule}^{-1} \cdot \text{s}^{-1}$ | $\text{OH} + \text{NO}_2 (+\text{N}_2)$ | $k_{\text{ClO}}/k_{\text{OH}}$ |
|----------------|------------------|---------------|------------------------------------|--|---|--------------------------------|
| 15 | 85.0 | 220 | 18.6 | 1.2 (-12) ^a | 1.0 (-11) ^d | 0.12 |
| 20 | 38.5 | 217 | 18.27 | 6.8 (-13) ^a | 6.6 (-12) ^d | 0.10 ₃ |
| 25 | 18.0 | 222 | 17.93 | 3.5 (-13) ^a | 3.6 (-12) ^d | 0.09 ₇ |
| 30 | 8.6 | 227 | 17.58 | 1.6 (-13) ^b | 1.7 (-12) ^d | 0.09 ₄ |
| 35 | 4.3 | 235 | 17.26 | 6.7 (-14) ^c | 7.6 (-13) ^e | 0.08 ₈ |
| 40 | 2.25 | 250 | 16.92 | 2.4 (-14) ^c | 3.4 (-13) ^e | 0.07 |
| 45 | 1.21 | 260 | 16.60 | 1.0 (-14) ^c | 1.5 (-13) ^e | 0.06 ₆ |
| 50 | 0.65 | 270 | 16.27 | 4.0 (-15) ^c | 6.0 (-14) ^e | 0.06 ₆ |

Figures in brackets are powers of ten.

^a 'Fall-off' calculation, this work. ^b Interpolated from 'falloff' curves in Figure 2. ^c Zahniser, Chang, Kaufman ³ (from measurements for $M = \text{He}$ and converted for $M = \text{N}_2$). ^d Anastasi, Smith ¹⁴. ^e Erler, Field, Zellner, Smith ¹⁵.

Table I. Effective bimolecular rate constants for $\text{ClO} + \text{NO}_2 (+\text{N}_2)$ and $\text{OH} + \text{NO}_2 (+\text{N}_2)$.

In order to illuminate the kinetic ranges in which these reactions take place in the stratosphere, it is useful to plot the effective bimolecular rate constants against stratospheric density (Figure 3). At low altitudes the kinetic regime for both reactions is that of the 'fall-off' curves at 220 K. With increasing altitude the kinetics becomes purely third-order. The effective rate constants, however, do not follow the $[\text{M}]$ proportional region of the 220 K 'fall-off' curve, due to a gradual increase in temperature.

Acknowledgement

The author should like to thank Prof. H. Gg. Wagner for his interest in this work and for stimulating

discussion. Thanks are also due to Prof. J. Troe for advice and help with the application of the theory.

Note added in proof: A 'fall-off' calculation for the title reaction was recently also carried out by Smith and Golden (G. P. Smith, D. M. Golden, *Int. J. Chem. Kin.*, in press). In their calculation the authors used RRKM theory in conjunction with a modified Gorin transition state. Although this theory predicts a larger k_1^∞ data, the derived fall-off behaviour at lower total pressures and therefore the effective rate constants under atmospheric conditions are in good agreement with the results from the present work.

- ¹ F. S. Rowland, J. E. Spencer, and M. J. Molina, *J. phys. Chem.* **80**, 2711 [1976].
- ² 'Halocarbons: Effect on Stratospheric Ozone.' Report of the National Academy of Sciences, Panel on Atmospheric Chemistry, Committee on Impact of Stratospheric Change, September 1976.
- ³ M. S. Zahniser, J. S. Chang, and F. Kaufman, *J. Chem. Phys.*, in press.
- ⁴ J. Birks et al., unpublished results, report to the Manufacturing Chemists Association.
- ⁵ M. T. Leu, C. L. Lin, and W. B. De More, *J. phys. Chem.* **81**, 190 [1977].
- ⁶ H. D. Knauth, private communication.
- ⁷ J. Troe, *Ber. Bunsenges. phys. Chem.* **78**, 478 [1974].
- ⁸ M. Quack and J. Troe, *Ber. Bunsenges. phys. Chem.* **81**, 329 [1977].
- ⁹ R. Zellner, submitted for publication.
- ¹⁰ H. D. Knauth, H. Martin, and W. Stockmann, *Z. Naturforsch.* **29 a**, 200 [1974].
- ¹¹ J. Shamir, D. Yelling, and H. H. Claasen, *Isr. J. Chem.* **12**, 1015 [1974].
- ¹² R. H. Miller, D. L. Bernitt, and I. C. Hisatsune, *Spectrochim. Acta* **23 A**, 223 [1967].
- ¹³ K. S. Pitzer, *Quantum Chemistry*, Prentice-Hall, Inc., New York 1953.
- ¹⁴ C. Anastasi and I. W. M. Smith, *J. Chem. Soc. Far. II*, **72**, 1459 [1976].
- ¹⁵ K. Erler, D. Field, R. Zellner, and I. W. M. Smith, *Ber. Bunsenges. Phys. Chem.* **81**, 22 [1977].